0026-895X/11/8002-228–239$25.00
MOLECULAR PHARMACOLOGY
Copyright © 2011 The American Society for Pharmacology and Experimental Therapeutics
Mol Pharmacol 80:228–239, 2011

Vol. 80, No. 2
72413/3699894
Printed in U.S.A.

Substrate Specificity and Ligand Interactions of CYP26A1, the Human Liver Retinoic Acid Hydroxylase

Jayne E. Thatcher, Brian Buttrick, Scott A. Shaffer, Jakob A. Shimshoni, David R. Goodlett, Wendel L. Nelson, and Nina Isoherranen

Departments of Pharmaceutics (J.E.T., B.B., J.A.S., N.I.) and Medicinal Chemistry (S.A.S., D.R.G., W.L.N.), School of Pharmacy, University of Washington, Seattle, Washington

Received March 21, 2011; accepted April 26, 2011

ABSTRACT

All-*trans*-retinoic acid (atRA) is the active metabolite of vitamin A. atRA is also used as a drug, and synthetic atRA analogs and inhibitors of retinoic acid (RA) metabolism have been developed. The hepatic clearance of atRA is mediated primarily by CYP26A1, but design of CYP26A1 inhibitors is hindered by lack of information on CYP26A1 structure and structure-activity relationships of its ligands. The aim of this study was to identify the primary metabolites of atRA formed by CYP26A1 and to characterize the ligand selectivity and ligand interactions of CYP26A1. On the basis of high-resolution tandem mass spectrometry data, four metabolites formed from atRA by CYP26A1 were identified as 4-OH-RA, 4-oxo-RA, 16-OH-RA and 18-OH-RA. 9-*cis*-RA and 13-*cis*-RA were also substrates of CYP26A1. Forty-two compounds with diverse structural properties were tested for CYP26A1 inhibition using 9-*cis*-RA as a probe, and IC_{50} values for 10 inhibitors were determined. The imidazole- and triazole-containing inhibitors [*S*-(*R**,*R**)]-*N*-[4-[2-(dimethylamino)-1-(1*H*-imidazole-1-yl)propyl]-phenyl]2-benzothiazolamine (R116010) and (*R*)-*N*-[4-[2-ethyl-1-(1*H*-1,2,4-triazol-1-yl)butyl]phenyl]-2-benzothiazolamine (R115866) were the most potent inhibitors of CYP26A1 with IC_{50} values of 4.3 and 5.1 nM, respectively. Liarozole and ketoconazole were significantly less potent with IC_{50} values of 2100 and 550 nM, respectively. The retinoic acid receptor (RAR) γ agonist CD1530 was as potent an inhibitor of CYP26A1 as ketoconazole with an IC_{50} of 530 nM, whereas the RARα and RARβ agonists tested did not significantly inhibit CYP26A1. The pan-RAR agonist 4-[(*E*)-2-(5,6,7,8-tetrahydro-5,5,8,8-tetramethyl-2-naphthalenyl)-1-propenyl]benzoic acid and the peroxisome proliferator-activated receptor ligands rosiglitazone and pioglitazone inhibited CYP26A1 with IC_{50} values of 3.7, 4.2, and 8.6 μM, respectively. These data demonstrate that CYP26A1 has high ligand selectivity but accepts structurally related nuclear receptor agonists as inhibitors.

Introduction

All-*trans*-retinoic acid (atRA) is the biologically active metabolite of vitamin A (retinol), but three other isomers of retinoic acid (9-*cis*-RA, 13-*cis*-RA, and 9,13-*dicis*-RA) can also be detected in vivo (Kane et al., 2008, 2010). During development, atRA regulates cell differentiation (Duester, 2008) and during adult life it is important for maintaining healthy epithelia, immunity, and fertility and for regulating cell proliferation (Blomhoff and Blomhoff, 2006). Retinoic acid isomers also play a role in adult neurogenesis and cell survival (Jacobs et al., 2006), and they contribute to regulation of glucose homeostasis (Kane et al., 2010). The many biological effects of atRA are believed to result from atRA binding to three nuclear retinoic acid receptors (RARα, RARβ, and RARγ), which are activated by RA isomers, resulting in induction of gene transcription (Petkovich et al., 1987; Altucci et al., 2007; Tang and Gudas, 2011). atRA, 9-*cis*-RA, and 13-*cis*-RA are all used clinically in treatment of various cancers and skin diseases, but the clinical use of endogenous retinoids has been limited because of side effects caused by

This work was supported by the National Institutes of Health National Institute of General Medical Sciences [Grants T32-GM007750, R01-GM081569, R01-GM081569-S1].
Article, publication date, and citation information can be found at http://molpharm.aspetjournals.org.
doi:10.1124/mol.111.072413.

ABBREVIATIONS: RA, retinoic acid; atRA, all-*trans*-retinoic acid; RAR, retinoic acid receptor; RAMBA, RA metabolism-blocking agent; R75251, 5-[(3-chlorophenyl)-1*H*-imidazol-1-ylmethyl]-1*H*-benzimidazole hydrochloride; P450, cytochrome P450; GW 9662, 2-chloro-5-nitro-*N*-phenylbenzamide; L-165,041, [4-[3-(4-acetyl-3-hydroxy-2-propylphenoxy)propoxy]phenoxy]acetic acid; AM 580, 4-[(5,6,7,8-tetrahydro-5,5,8,8-tetramethyl-2-naphthalenyl)carboxamido]benzoic acid; CS5, 2-[1-(4-hydroxyphenyl)methylidene]-3,4-dihydro-2*H*-napthalen-1-one; CS6, 2-(4-hydroxybenzyl)-6-methoxy-3,4-dihydro-2*H*-napthalen-1-one; R115866, (*R*)-*N*-[4-[2-ethyl-1-(1*H*-1,2,4-triazol-1-yl)butyl]phenyl]-2-benzothiazolamine; R116010, [*S*-(*R**,*R**)]-*N*-[4-[2-(dimethylamino)-1-(1*H*-imidazole-1-yl)propyl]-phenyl]-2-benzothiazolamine; TTNPB, 4-[(*E*)-2-(5,6,7,8-tetrahydro-5,5,8,8-tetramethyl-2-naphthalenyl)-1-propenyl]benzoic acid; AC55649, 4′-octyl-[1,1′-biphenyl]4-carboxylic acid; CD1530, 4-(6-hydroxy-7-tricyclo[3.3.1.13,7]dec-1-yl-2-naphthalenyl)benzoic acid; HPLC, high-performance liquid chromatography; MS/MS, tandem mass spectrometry; MRM, multiple reaction monitoring; PPAR, peroxisome proliferator-activated receptor; LC, liquid chromatography; AUC, area under the curve.

off-target effects and development of resistance (Altucci et al., 2007; Garattini et al., 2007).

Resistance to atRA treatment in cancer therapy is attributed to increased systemic clearance and cellular metabolism of atRA during treatment (Muindi et al., 1992; van der Leede et al., 1997). To improve therapeutic outcomes, synthetic RA analogs, RAR agonists, and RA metabolism-blocking agents (RAMBAs) have been developed and tested for treatment of cancers and skin diseases (Njar et al., 2006; Altucci et al., 2007). The first tested inhibitors of atRA metabolism included liarozole (5-[(3-chlorophenyl)-1*H*-imidazol-1-ylmethyl]-1*H*-benzimidazole hydrochloride, R75251) and ketoconazole that inhibited metabolism of atRA in vivo in rats and in in vitro models (Van Wauwe et al., 1988, 1990; Wouters et al., 1992). Subsequently, more specific and potent inhibitors of atRA metabolism synthesized by several groups showed potential for treatment of cancers and skin diseases in both in vitro and in vivo models (Patel et al., 2004; Mulvihill et al., 2005; Yee et al., 2005; Njar et al., 2006).

CYP26A1 appears to be a likely target for development of new inhibitors of atRA metabolism. It is likely that CYP26A1, a P450 identified as an RA hydroxylase that is up-regulated by atRA (White et al., 1996), is induced during atRA treatment. atRA has high affinity for and is efficiently metabolized by CYP26A1 (Lutz et al., 2009), and CYP26A1 is the primary enzyme responsible for hepatic clearance of atRA (Thatcher et al., 2010). CYP26A1 is also inducible by atRA in human liver (Tay et al., 2010). However, neither the structure of CYP26A1 nor the structural requirements of potent CYP26A1 binding are well characterized. Three homology models of CYP26A1 have been reported (Gomaa et al., 2006; Ren et al., 2008; Karlsson et al., 2008) on the basis of the crystal structures of CYP3A4, CYP2C8, CYP2C9, and CYP51. However, experimental data on ligand overlap, atRA binding orientations, and metabolite identification are not available to support the construction of these models, perhaps because of a lack of a system to screen CYP26A1 ligands. Use of atRA as a substrate to screen CYP26A1 inhibitors is not feasible in cell systems and with recombinant CYP26A1, because the primary metabolites are rapidly depleted, making measurements of catalytic activity confounding. In addition, atRA binds CYP26A1 with high affinity (K_m = 9.3 nM) (Lutz et al., 2009), requiring very sensitive assays to measure product formation if substrate is added at the K_m or lower concentration. Therefore, an alternative substrate for CYP26A1 is needed. In this study, 9-*cis*-RA was evaluated as an alternative substrate for inhibitor screening, the specific metabolites of atRA and 9-*cis*-RA formed by CYP26A1 were identified, and the overall ligand selectivity of CYP26A1 was established. The data obtained will be valuable for rationalization of observed in vivo interactions between xenobiotics and atRA, for design of new CYP26A1 inhibitors, and for refining features of existing homology models of CYP26A1.

Materials and Methods

Chemicals. atRA, 9-*cis*-RA, acitretin, 2-chloro-5-nitro-*N*-phenylbenzamide (GW 9662), [4-[3-(4-acetyl-3-hydroxy-2-propylphenoxy)propoxy]-phenoxy]acetic acid (L-165,041), 4-[(5,6,7,8-tetrahydro-5,5,8,8-tetramethyl-2-naphthalenyl)carboxamido]benzoic acid (AM 580), ketoconazole, itraconazole, fluconazole, quinapril, propranolol, methoxypsoralen, quinidine, omeprazole, diltiazem, erythromycin, paclitaxel, pimozide, ranolazine, terfenadine, verapamil, simvastatin, danazol, and NADPH were purchased from Sigma-Aldrich (St. Louis, MO). Cyclosporine and tamoxifen were purchased from Enzo Life Sciences International, Inc. (Plymouth Meeting, PA). Voriconazole was a gift from Dr. Kenneth E. Thummel, University of Washington (Seattle, WA). 2-[1-(4-Hydroxyphenyl)methylidene]-3,4-dihydro-2*H*-napthalen-1-one (CS5) and 2-(4-hydroxybenzyl)-6-methoxy-3,4-dihydro-2*H*-napthalen-1-one (CS6) were gifts from Dr. Claire Simons (Medicinal Chemistry, Welsh School of Pharmacy, Cardiff University, Cardiff, UK). (*R*)-*N*-[4-[2-ethyl-1-(1*H*-1,2,4-triazol-1-yl)butyl]phenyl]-2-benzothiazolamine (R115866) and R116010 were gifts from Johnson & Johnson (Beerse, Belgium). Liarozole, TTNPB, 4′-octyl-[1,1′-biphenyl]-4-carboxylic acid (AC55649), and 4-(6-hydroxy-7-tricyclo[3.3.1.13,7]dec-1-yl-2-naphthalenyl)benzoic acid (CD1530) were purchased from Tocris Bioscience (Ellisville, MO). atRA-d_5 was purchased from Santa Cruz Biotechnology, Inc. (Santa Cruz, CA). Rosiglitazone was purchased from Cayman Chemical (Ann Arbor, MI), and pioglitazone was purchased from Altan Biochemicals (Orange, CT). 3-OH-retinal and 4-OH-9-*cis*-RA were purchased from Toronto Research Chemicals Inc. (North York, ON, Canada). The protease inhibitors used in this study were obtained from the National Institutes of Health AIDS Research and Reference Reagent Program (Germantown, MD). CYP26A1 was expressed in Sf9 cells as described previously and used as microsomal fractions supplemented with rat P450 reductase expressed in *Escherichia coli* (Lutz et al., 2009). All solvents used were HPLC grade or higher and were purchased from EMD Chemicals (Gibbstown, NJ), Mallinckrodt Baker, Inc. (Phillipsburg, NJ), or Thermo Fisher Scientific (Waltham, MA).

Synthesis of 3-OH-atRA. 3-OH-atRA was synthesized by oxidation of 3-OH-retinal with Tollens' reagent (Barua and Barua, 1964). The Tollens' reagent was freshly prepared before use by mixing equal volumes of 10% w/w $AgNO_3$ and 10% w/w NaOH. Ammonium hydroxide solution (Sigma-Aldrich) was added dropwise to dissolve the precipitated Ag_2O. Tollens' reagent (1 ml) was added slowly to 3 mg of 3-OH-retinal dissolved in 8 ml of methanol and stirred for 6 h at 37°C. The reaction was quenched by acidification with aqueous 0.5 N HCl. The product was extracted with dichloromethane, dried over Na_2SO_4, and evaporated to dryness. The identity of the product was verified by NMR analysis. ^{1}H-NMR (500 MHz, $CDCl_3$) δ 0.97 (s, 3H, 16-CH_3), 0.98 (s, 3H, 17-CH_3), 1.76 (s, 3H, 18-CH_3), 2.04 (s, 3H, 19-CH_3), 2.38 (s, 3H, 20-CH_3), 4.03 (t, 1H, 3-H), 5.83 (s, 1H, 14-H), 6.09 (d, 1H, 8-H), 6.19 (d, 1H, 10-H), 6.27 (d, 1H, 12-H), 6.35 (d, 1H, 7-H), 7.05 (dd, 1H, 11-H). The product was also analyzed by HPLC-UV as described below for hydroxylated metabolites and had a retention time of 14.9 min, 0.8 min before the 4-OH-RA standard that eluted at 15.7 min.

Incubation Conditions and HPLC Analysis for RA Isomers. Unless otherwise described, incubations were performed with 5 pmol of CYP26A1 and 10 pmol of P450 reductase. The purified rat reductase was added to CYP26A1 microsomes, and the reductase was allowed to incorporate into the membrane for 10 min at room temperature. The final volume of each incubation sample was then brought to 1 ml by adding 100 mM potassium phosphate buffer, pH 7.4, 9-*cis*-RA, and, where appropriate, inhibitor or solvent. Compounds were dissolved in methanol or dimethyl sulfoxide, and final solvent amounts in the incubations were kept at 1%. The samples were preincubated for 5 min at 37°C before the reaction was initiated with 1 mM NADPH. Unless otherwise noted, incubation times were 1 min. Extraction of RA and its metabolites, followed by HPLC analysis, was performed as published previously (Thatcher et al., 2010). In brief, incubations were terminated with 5 ml of ethyl acetate, and acitretin was added as an internal standard. The ethyl acetate layer was evaporated and reconstituted in methanol. Analytes were separated by HPLC and detected with a multiple wavelength detector, monitoring at 360 nm. Data analysis was performed using HP Chemstation software.

Characterization of atRA and 9-*cis*-RA Metabolism by CYP26A1. To determine whether other RA isomers (9-*cis*-RA and 13-*cis*-RA) are substrates of CYP26A1 and to identify the metabolites formed from atRA and 9-*cis*-RA by CYP26A1, 9-*cis*-RA, atRA-d_5, and atRA were incubated at 100 μM concentrations in the presence of 100 pmol of CYP26A1 and 200 pmol of reductase for 1 h. The structures of these compounds are shown in Fig. 1. In addition, 9-*cis*-RA, 13-*cis*-RA, and atRA were incubated at a 500 nM concentration in the presence of 5 pmol of CYP26A1 and 10 pmol of P450 reductase for 2 min. Samples were analyzed by HPLC as described above. Fractions from the incubations performed with 100 μM substrate were collected for mass spectrometric analysis. Full-scan and tandem mass spectra were acquired on an LTQ-Orbitrap (Thermo Fisher Scientific) hybrid mass spectrometer operated in the negative ion electrospray mode. Fractions were introduced by infusion using a NanoAcquity ultra-high-performance liquid chromatograph (Waters, Milford, MA) interfaced to a CaptiveSpray (Michrom Bioresources, Auburn, CA) ion source. Samples were injected in 10 μl and infused in a 1:1 mixture of water-acetonitrile containing 0.1% formic acid (v/v) flowing at 5 μl/min. Full-scan mass spectra were acquired in the Orbitrap at 60,000 resolution. Collision-induced dissociation occurred in the LTQ using a normalized collision energy of 35% and an isolation width of 4 Da, but with the resulting tandem mass spectra acquired in the Orbitrap at 15,000 resolution. Data-dependent parameters were programmed to allow a cycle of one mass spectrum followed by tandem mass spectra of the three most abundant ions. All other data-dependent parameters were minimized to allow for maximal data redundancy (i.e., scan averaging). Data analysis of MS/MS fragments was performed with Xcalibur software (Thermo Fisher Scientific).

The metabolites of 9-*cis*-RA were further characterized using an API5500 Q/LIT mass spectrometer (AB SCIEX, Foster City, CA) equipped with a 1290 Infinity UPLC (Agilent Technologies, Santa Clara, CA) and Zorbax C18 column (3.5 mm, 2.1 × 100 mm; Agilent Technologies). The metabolites were separated using gradient elution from 90% acetonitrile and aqueous 10% ammonium acetate (50 mM) to 90% acetonitrile over 15 min. The column was maintained at 25°C, and the injection volume was 10 μl. Negative ion electrospray was used, and the ion source voltage (internal standard) and source temperature were set at −4500 V and 400°C, respectively. The MRM transitions of m/z = 315 > 253 Da and m/z = 315 > 241 Da were monitored. For both transitions, the declustering potential, collision energy, and collision exit potential were set to −90, −25, and −10 V, respectively. In parallel, daughter ion scans of m/z = 315 were collected from 100 to 350 m/z. The detection settings for the scan parameters were identical to those for MRM runs.

Determination of Kinetic Constants of 9-*cis*-RA Metabolism by CYP26A1. The affinity of 9-*cis*-RA to CYP26A1 was determined by conducting a Michaelis-Menten kinetic analysis of formation of the primary metabolites. After it was established that product formation was linear with time and the protein concentration used, incubations were performed with 11 different concentrations of 9-*cis*-RA, between 25 nM and 1 μM. Peak area ratios (primary metabolites quantified as a single peak to internal standard) were plotted against the initial substrate concentrations, and the Michaelis-Menten equation was fit to the data using GraphPad Prism (GraphPad Software Inc., San Diego, CA). The K_m value was obtained from the fit, but the V_{max} was not determined because the amount of products formed could not be quantified in the absence of reference materials.

Identification of CYP26A1 Ligands and Calculation of IC_{50} Values. Forty-two compounds, as listed in Table 1, were tested as potential inhibitors of CYP26A1. Compounds selected included

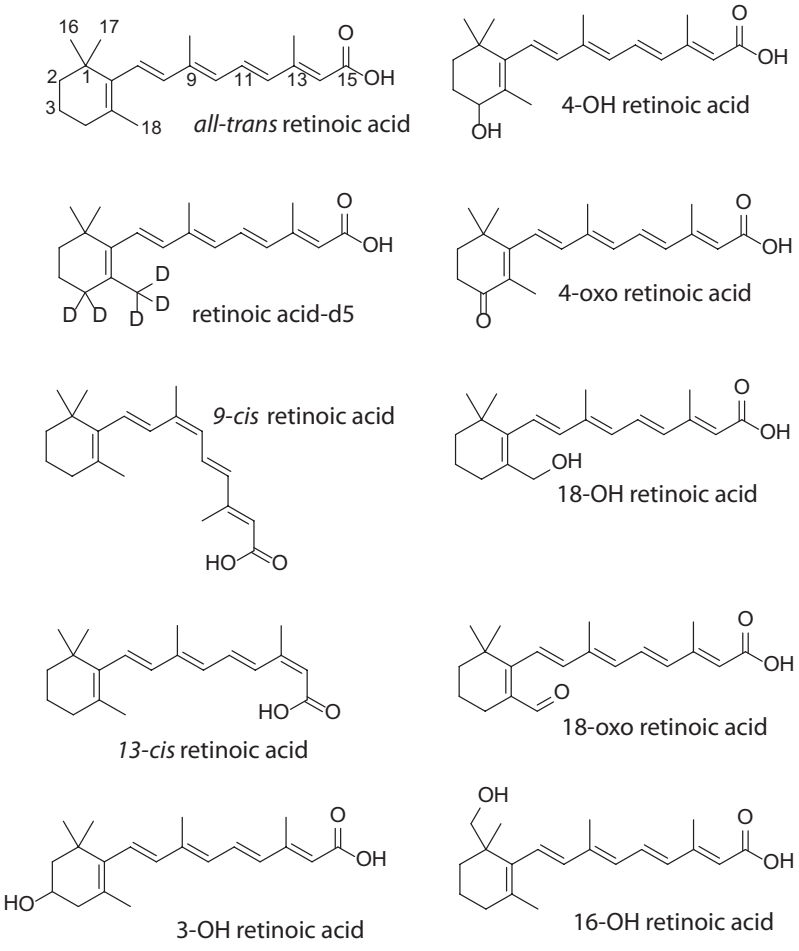

Fig. 1. Chemical structures of RA isomers, atRA-d_5, and detected or proposed atRA metabolites.

PPAR and RAR agonists, published RAMBAs, and known P450 inhibitors and probes with wide structural variability, including azole antifungals. Compounds were first tested for inhibition of CYP26A1-mediated 9-*cis*-RA hydroxylation at a 10 μM concentration. Because of poor ligand solubility, the protease inhibitors were tested at 5 μM. The formation of the primary hydroxylated 9-*cis*-RA metabolite eluting at retention time 16.4 min was monitored as a measure of CYP26A1 activity. The percentage remaining activity for each inhibitor was calculated by comparing the observed hydroxylation in the test incubations to that measured in controls containing an equal volume of the same solvent as the one in which the inhibitor was dissolved. All incubations were performed in triplicate. To confirm a lack of interference from either the inhibitor or potential metabolites of the inhibitor in the HPLC analysis, the inhibitors were incubated with 5 pmol of CYP26A1, 10 pmol of reductase, and 1 μM concentrations of each ligand for 1 min in the presence and absence of NADPH and analyzed by HPLC, monitoring wavelengths 360, 280, and 250 nm.

Compounds that showed >10% inhibition of CYP26A1 mediated 9-*cis*-RA hydroxylation at 10 μM concentration were also tested at 1 μM to rank the inhibitory effects of the ligands tested and to estimate initial inhibitory potency. IC_{50} values were determined for those compounds that inhibited CYP26A1 activity by more than 50% at a 10 μM concentration and showed greater than 10% inhibition at a 1 μM concentration. For IC_{50} determination, at least five concentrations spanning above and below the predicted IC_{50} were tested, and each concentration was analyzed in duplicate. The IC_{50} values were determined by nonlinear regression using GraphPad Prism, according to eq. 1:

$$100\% \cdot \frac{v_i}{v} = \left(\frac{v_i}{v}\right)_{min} \cdot 100\% + \frac{((v_i/v)_{max} - (v_i/v)_{min} \cdot 100\%)}{(1 + 10^{(I - \log IC_{50})})} \quad (1)$$

in which $100\% \cdot (v_i/v)$ is the percentage of activity remaining, $(v_i/v)_{max} \cdot 100\%$ is the fitted percentage maximum activity remaining, and $(v_i/v)_{min} \cdot 100\%$ is the percentage minimum activity remaining. For compounds with IC_{50} values less than 100 nM, all fits were corrected for inhibitor depletion, and the K_d was determined using the Morrison equation as described in eq. 2:

$$[EI] = \frac{[E] + [I] + K_d - \sqrt{([E] + [I] + K_d)^2 - 4[E][I]}}{2} \quad (2)$$

TABLE 1
Summary of compounds screened as potential inhibitors of CYP26A1
Compounds were assigned as "positive" if they inhibited CYP26A1 more than 10% when tested at 10 μM.

Screen-Positive	Screen-Negative
R115866	AC 55649
R116010	Nelfinavir
Liarozole	Quinidine
Ketoconazole	Lopinavir
Fluconazole	Simvastatin
Itraconazole	Diltiazem
Voriconazole	Methoxypsoralen
Terfenadine	Darunavir
Danazol	Erythromycin
Tamoxifen	Verapamil
Pimozide	Propranolol
Tipranavir	Atazanavir
CS6	Omeprazole
CS5	Indinavir
CD 1530	Saquinavir
TTNPB	Ranolazine
L-165,041	Paclitaxel
Rosiglitazone	Cyclosporine
Pioglitazone	Quinapril
AM 580	Amprenavir
GW 9662	Ritonavir

in which K_d is the affinity constant of the inhibitor, [*I*] is the concentration of inhibitor, [*E*] is the concentration of enzyme, and [*EI*] is the concentration of the enzyme-inhibitor complex.

Determination of Ligand-Induced Binding Spectra and Spectral Binding Constants. To determine whether the inhibitors identified bind within the active site of CYP26A1, ligand-induced binding spectra were measured with R115866, R116010, and ketoconazole. For these studies, a 1-ml sample of 0.2 μM CYP26A1 microsomes in 100 mM potassium phosphate buffer was split between the sample and reference cuvettes, and the binding spectra were measured using an Aminco DW2 dual-beam spectrophotometer (Olis Instruments, Bogart, GA), scanning from 500 to 375 nm. The inhibitor of interest was added to the sample cuvette until a difference spectrum was observed. An equal volume of solvent was added to the control cuvette. R116010 was tested at 4, 8, 12, 16, and 20 μM, and R115866 was tested at 0.2, 0.4, 0.6, 1, 1.2, 1.4, 1.6, 3.6, and 5.2 μM. Ketoconazole was tested at 20, 40, 60, 80, 100, and 120 μM. The absorbance spectra were normalized to 420 or 490 nm for comparison of the difference spectra obtained.

Results

Characterization of atRA and 9-*cis*-RA Metabolism by CYP26A1. To identify the primary metabolites formed by CYP26A1, atRA, atRA-d_5, and 9-*cis*-RA (Fig. 1) were incubated with CYP26A1. Metabolite formation was analyzed by HPLC-UV and individual metabolite peaks detected were collected as HPLC fractions. Molecular ion and MS/MS fragmentation data were collected for each fraction at high mass accuracy (0.3–4 ppm accuracy). Four primary metabolites (peaks 1–4) were formed from atRA by CYP26A1 (Fig. 2). Three of the atRA metabolites (peaks 1, 3, and 4) had an [M − H] ion of 315.196 *m/z*, suggesting that these were hydroxylated metabolites. Two of these metabolites (peaks 1 and 4) lost a deuterium as a result of hydroxylation of atRA-d_5, giving a [M − H] ion of 319.221 *m/z*. This observation suggests that peaks 1 and 4 correspond to hydroxylations at the deuterated carbons, C-4 or C-18. Because the retention time of peak 1 was identical to that of the synthetic 4-OH-atRA, it was identified as 4-OH-atRA and peak 4 was identified as 18-OH-atRA. The third hydroxylation product (peak 3) resulted from a hydroxylation in nondeuterated carbon because in the incubation of atRA-d_5, the [M − H] ion was 320.227 *m/z*. The hydroxylation is probably on the β-ionone ring at C-3 or C-16. The synthetic reference material of 3-OH-atRA eluted at 14.9 min (before 4-OH-atRA at 15.8 min; data not shown), and hence peak 3 could not be 3-OH-atRA. The dominant MS/MS fragment from peak 3 in atRA incubations ([M − H] 315.196 *m/z*) was 241.196 *m/z* in addition to the characteristic loss of CO_2 (loss of 43.989) and H_2O (loss of 18.010) (Fig. 2). The 241.196 *m/z* fragment was attributed to the loss of formaldehyde (loss of 30.010) from the 271.206 *m/z* ion instead of ethane, which would be a loss of 30.046. The 241.196 *m/z* ion is absent from the 4-OH-atRA MS/MS spectrum, which is dominated by a loss of CO_2 (loss of 43.989) and loss of H_2O (loss of 18.010), resulting in fragments at 253.196 *m/z*, 271.206 *m/z*, and 297.186 *m/z* (Fig. 2). However, the 241.196 *m/z* fragment is a minor fragment in the MS/MS spectrum of 18-OH-atRA. In the MS/MS spectrum of peak 3 from atRA-d_5 incubation, the corresponding fragment is 246.227, retaining all five deuteriums, suggesting a loss of formaldehyde from an undeuterated carbon. The loss of formaldehyde is most likely favored for hydroxylations of a methyl group (C-16 or C-18) in contrast to hydroxylation of the

carbons in the β-ionone ring. Based on these data, peak 3 was identified as the 16-OH-atRA. The fourth metabolite, peak 2, had an [M − H] of 313.180 *m/z*, suggesting that it is a ketone or an aldehyde. The corresponding metabolite from atRA-d_5 had an [M − H] 316.20 *m/z*, suggesting that the ketone or aldehyde was at a deuterated position, C-4 or C-18. This metabolite has a retention time similar to that of synthetic 4-oxo-RA, and no loss of formaldehyde was detectable in the MS/MS fragmentation. Loss of formaldehyde would be expected for the 18-oxo-RA. Instead, a loss of a CH_3 is detected in the metabolite formed from atRA (loss of 15.02 from 269.191 *m/z*) and a loss of CD_3 in the metabolite formed in the incubation with atRA-d_5 (loss of 18.042 from 272.209 *m/z*), resulting in the common MS/MS fragment of 254.167 *m/z*. This data suggest that peak 2 is the 4-oxo-atRA.

All three RA isomers tested, atRA, 9-*cis*-RA, and 13-*cis*-RA, were found to be substrates of CYP26A1. No metabolites were observed in the absence of NADPH, absence of protein, or absence of substrate. In incubations with 13-*cis*-RA, substantial isomerization was observed, preventing characterization of the hydroxylation kinetics of 13-*cis*-RA (data not shown). In contrast, 9-*cis*-RA underwent minimal isomerization during incubations. A metabolite at the same retention time as 4-OH-9-*cis*-RA reference material was detected

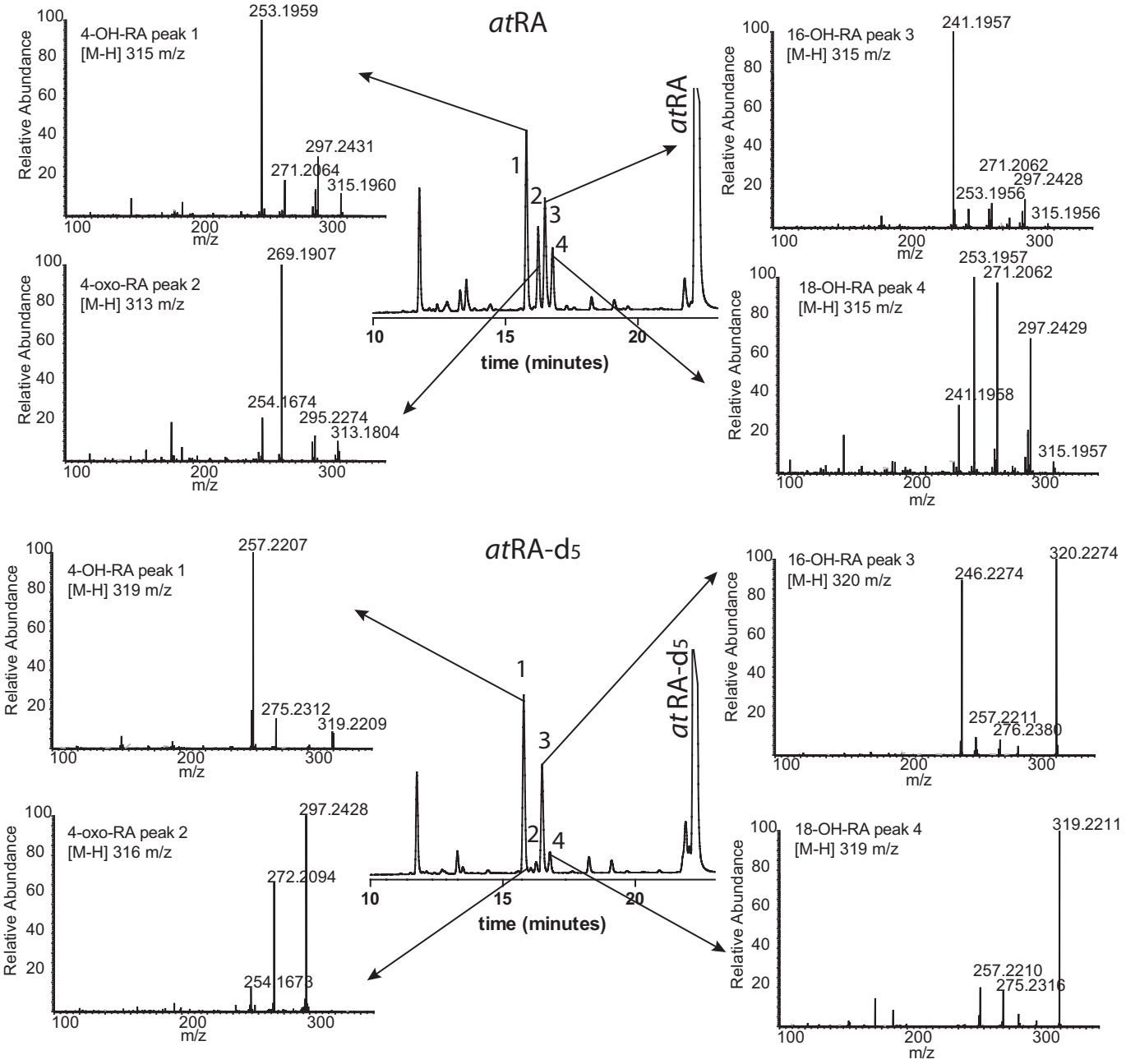

Fig. 2. Characterization of metabolites of atRA formed by CYP26A1. HPLC-UV chromatograms of the metabolites formed after incubation of atRA (top) or atRA-d_5 (bottom) at a 100 μM concentration with 100 pmol of CYP26A1 for 1 h. The peaks labeled as 1, 2, 3, and 4 were collected as HPLC fractions and analyzed by high-resolution mass spectrometry as described under *Materials and Methods*. The MS/MS spectra of the four fractions are shown with the [M − H] ion *m/z* listed as an inset to the spectrum. The four metabolites were identified as follows: peak 1, 4-OH-atRA; peak 2, 4-oxo-atRA; peak 3, 16-OH-atRA; and peak 4, 18-OH-atRA.

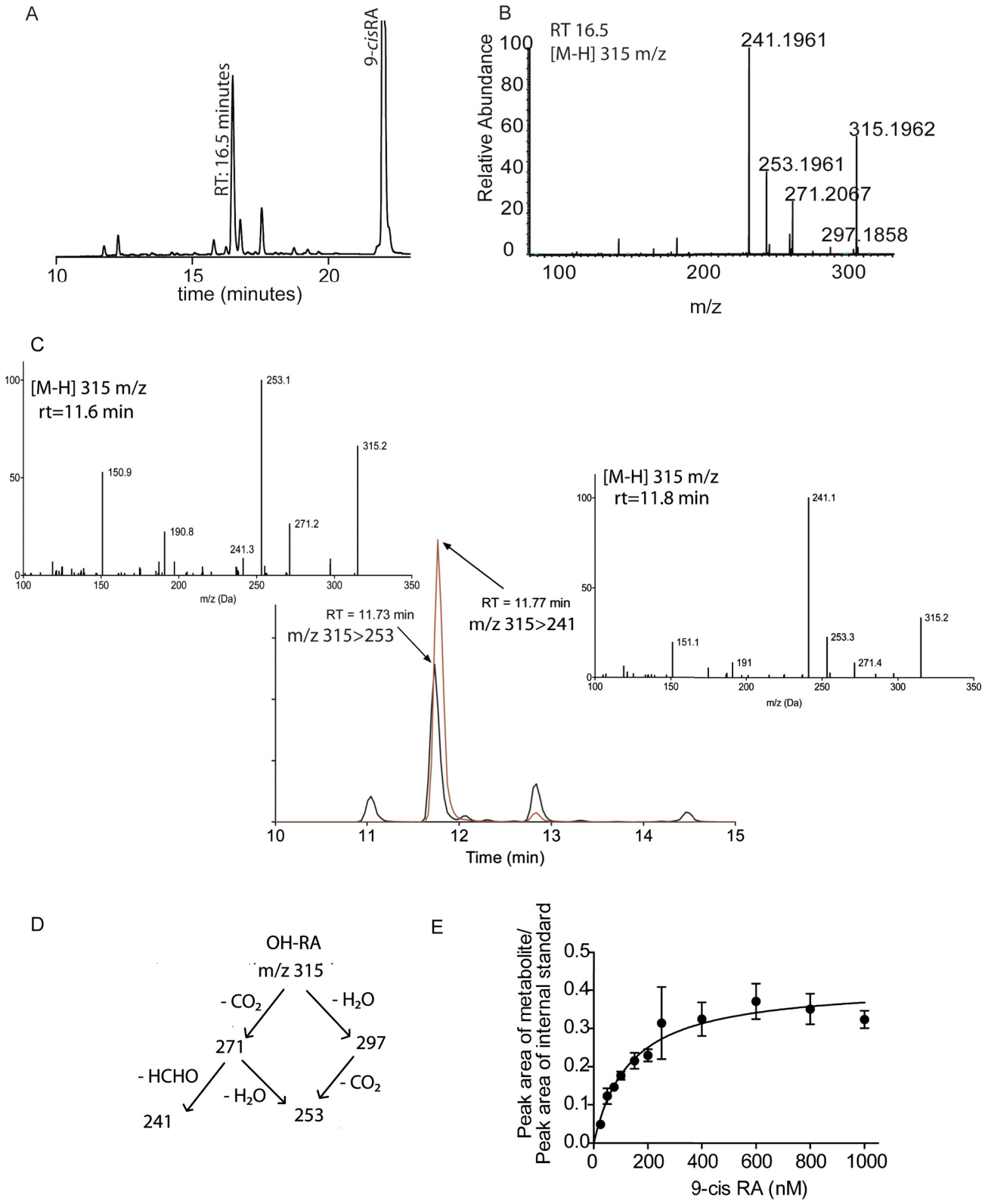

Fig. 3. Characterization of 9-*cis*-RA as a substrate of CYP26A1. A, an HPLC chromatogram of the metabolites formed from 9-*cis*-RA (100 μM) with 100 pmol of CYP26A1. The peak at 16.5 min depicted in A was collected for MS/MS analysis. B, the high-resolution MS/MS spectrum of [M − H] 315 *m/z* of this peak. C, further characterization of the 9-*cis*-RA metabolites detected by LC-MS/MS as described under *Materials and Methods*. The black trace shows the MRM chromatogram of *m/z* transition 315 > 253, and the red trace shows the *m/z* transition 315 > 241. Retention times (RT, rt) are not comparable between A and C because of the different HPLC separation conditions used. Insets, MS/MS spectra acquired from *m/z* 315 for the two overlapping peaks, demonstrating the presence of two different metabolites. D, proposed fragmentation pathway of the hydroxylated 9-*cis*-RA metabolites. E, determination of the Michaelis-Menten constant (K_m) for 9-*cis*-RA hydroxylation by CYP26A1 using 5 pmol of CYP26A1, 10 pmol of reductase, and 9-*cis*-RA concentrations from 25 nM to 1 μM. Incubation times were 1 min. The K_m was determined to be 134 nM.

(Fig. 3A), and minimal secondary metabolism from 9-*cis*-RA was observed. Mass spectrometric analysis of the LC fraction of the peak at a retention time of 16.5 min showed an [M − H] molecular ion at 315.196 *m/z*, confirming that this peak is a hydroxylation product. However, the MS/MS fragmentation data of the metabolite (Fig. 3B) showed a significant fragment at 241.196 *m/z,* a fragment that is absent from synthetic 4-OH-9-*cis*-RA (data not shown), but the main fragment in the proposed 16-OH-atRA. To further characterize this metabolite, LC-MS/MS analysis was used, monitoring two MRM transitions: 315 > 253 *m/z* and 315 > 241 *m/z* (Fig. 3C). This analysis allowed separation of two main metabolites from 9-*cis*-RA. The first one was mainly detected at the 315 > 253 channel and had an MS/MS fragmentation pattern of the 315 *m/z* identical to that of synthetic 4-OH-9-*cis*-RA (Fig. 3C). The second metabolite was detected mainly on the 315 > 241 channel and had a fragmentation pattern similar to that of the tentatively identified 16-OH-atRA (Fig. 3C). On the basis of these data, it was concluded that at least two hydroxylation products are formed from 9-*cis*-RA by CYP26A1, and the high-resolution MS/MS spectrum is a combination of two coeluting metabolites. The overall fragmentation pattern for the hydroxylated metabolites is shown in Fig. 3D.

Identification of CYP26A1 Inhibitors and Determination of IC_{50} Values. The apparent K_m for 9-*cis*-RA metabolism by CYP26A1 was determined to establish an appropriate substrate concentration for the inhibition assay (Fig. 3E). The K_m for the formation of the hydroxylated metabolites (quantified by UV as a single peak) of 9-*cis*-RA was 134 ± 30 nM. Based on this experimentally determined K_m, further incubations to identify and characterize potential inhibitors were performed at 100 nM 9-*cis*-RA.

Forty-two compounds were screened for CYP26A1 inhibition (Table 1). Twenty-one of these compounds resulted in >10% inhibition of 9-*cis*-RA hydroxylation at 10 μM concentration (Fig. 4, A and B). Eleven of these 21 compounds also inhibited CYP26A1 by >10% at 1 μM (Fig. 4, C and D). IC_{50} values (Table 2) were determined for all compounds that had >20% inhibition at 1 μM and for CS5, pioglitazone, and rosiglitazone.

The two compounds that were designed as inhibitors of atRA metabolism, R116010 and R115866 (Fig. 5), were the most potent inhibitors of CYP26A1 with low nanomolar K_d values (Table 2; Fig. 5). The IC_{50} value of ketoconazole (IC_{50} = 0.5 μM) was approximately 100-fold higher, and the IC_{50} of liarozole (IC_{50} = 2.1 μM) was approximately 500-fold higher than those of R115866 and R116010 (Table 2; Fig. 5). The IC_{50} values of other azoles (fluconazole, itraconazole, and voriconazole) appeared to be >10 μM, based on the <50% inhibition at a 10 μM concentration. The two inhibitors of RA metabolism lacking triazole or imidazole groups, CS5 and CS6 (Fig. 6), were less potent inhibitors of CYP26A1 than R115866, R116010, and ketoconazole, but CS5 had an IC_{50} similar to that of liarozole.

Some of the RAR agonists tested also bound to CYP26A1 and inhibited the hydroxylation of 9-*cis*-RA, but large differences in the binding affinity of the RAR agonists were observed. Of the RAR agonists tested, the most potent inhibitor was CD1530 (IC_{50} = 0.5 μM), an RARγ-selective agonist (Table 2; Fig. 6), which was equipotent with ketoconazole. TTNPB, a pan-RAR agonist, had a 10-fold higher IC_{50} (3.7 μM) as a CYP26A1 inhibitor than CD1530, and the RARβ selective agonist AC55649 did not inhibit CYP26A1 even at a 10 μM concentration. AM 580, an RARα-specific agonist, inhibited CYP26A1 by 58% at a 10 μM concentration but not at all at 1 μM. The two PPARγ agonists rosiglitazone and pioglitazone and the PPARβ/δ-selective agonist L-165,041 inhibited CYP26A1 with approximately equal potency, with IC_{50} values between 1.7 and 8.6 μM (Fig. 6). However, the PPARγ-selective irreversible antagonist GW 9662 did not have appreciable effects on CYP26A1 activity at 10 μM, despite the shared PPAR binding affinity.

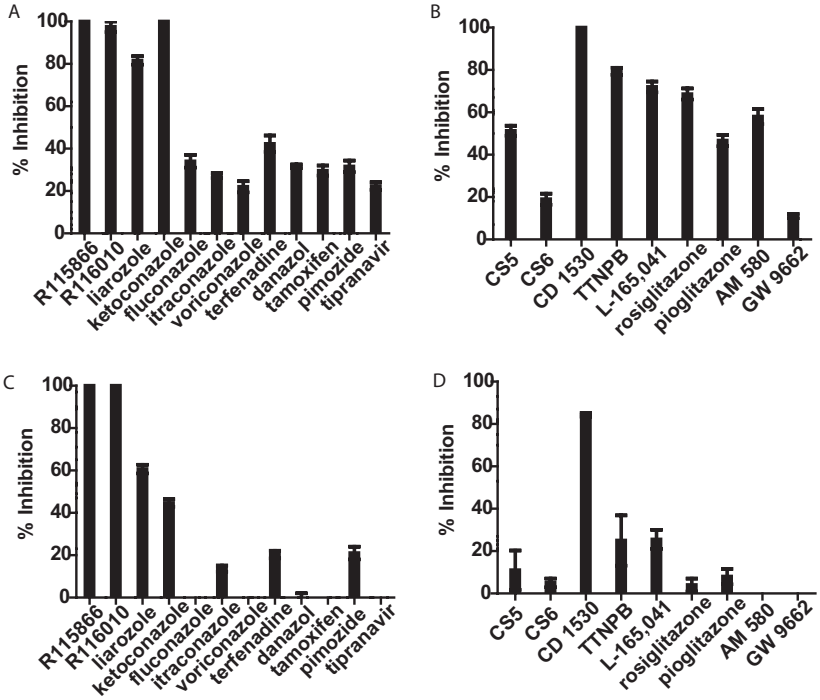

Fig. 4. Percentage inhibition of CYP26A1-mediated 9-*cis*-RA hydroxylation by identified ligands. The inhibition of CYP26A1 by a diverse selection of compounds (A and C) and select retinoids, RAMBAs, and RAR agonists (B and D). A and B show the inhibition at 10 μM inhibitor concentration, and C and D show inhibition at 1 μM inhibitor concentration with 9-*cis*-RA (100 nM) as substrate.

Determination of Ligand-Induced Binding Spectra. To determine whether the identified azole inhibitors bind within the CYP26A1 active site and whether a triazole or imidazole nitrogen coordinates to the heme iron, ligand-induced binding spectra were obtained using CYP26A1 insect cell microsomes (Fig. 7). R115866, R116010, and ketoconazole binding resulted in a type II binding spectrum characterized by a high to low spin shift of the heme iron. It is interesting to note that the minima and maxima of these spectra were shifted toward longer wavelengths compared with classic type II spectra. The observed minima were between 400 and 415 nm, the maxima were between 425 and 440 nm, and they increased with increasing concentrations.

Discussion

CYP26A1 is one of the main enzymes responsible for atRA hydroxylation, but the metabolites generated from atRA by CYP26A1 have been only partially identified (White et al., 1997; Chithalen et al., 2002; Lutz et al., 2009). This study showed that 4-OH-atRA and 18-OH-atRA as well as 4-oxo-atRA, are formed by CYP26A1. This is in agreement with previous data obtained from cell culture systems (Chithalen et al., 2002). However, in contrast with previously proposed formation of 3-OH-atRA, our data show that 3-OH-atRA is not a metabolite formed by CYP26A1 but instead that 16-OH-atRA is the most likely third hydroxylation product. 16-OH-atRA has been reported to be the main atRA hydroxylation product formed by CYP120A1, the cyanobacterial atRA hydroxylase homologous to CYP26A1 (Alder et al., 2009). 16-OH-atRA was also shown to be a metabolite of atRA in atRA-induced T47D cells, and its formation was inhibited by R116010 (Van Heusden et al., 2002). The oxidation of C16 probably results from rotation of the bond connecting the β-ionone ring to the linear isoprenoid side chain, placing the C16 near the heme similar to C4. This orientation is shown in the crystal structure of CYP120A1 in which C16 is at 4.4 Å from the heme (Kühnel et al., 2008). In a previous study, 4-oxo-atRA was not detected as a metabolite in incubations of 4-OH-atRA and CYP26A1 (Lutz et al., 2009). Hence, it is surprising that 4-oxo-atRA was detected in the current study. Further studies of the sequential dissociative and nondissociative metabolism of atRA by CYP26A1 are needed to explain this discrepancy.

In addition to atRA, 9-*cis*-RA was a substrate of CYP26A1, which is in contrast to the lack of hydroxylation of 9-*cis*-RA in transfected HCT 116-hCYP26 cells (Sonneveld et al., 1998). 9-*cis*-RA is a substrate of CYP26C1 (Taimi et al., 2004) with the 4-OH-9*cis*-RA identified as the main metabolite. The metabolism of 9-*cis*-RA by CYP26A1 also resulted in formation of 4-OH-9*cis*-RA, but the high-resolution MS/MS data as well as the LC-MS/MS data show that a second hydroxylation product, most likely 16-OH-9-*cis*-RA, is formed. Of interest, despite the high affinity of 9-*cis*-RA and atRA to CYP26A1 and the ligand selectivity of CYP26A1, multiple hydroxylation products are observed from both 9-*cis*-RA and atRA,

TABLE 2
IC_{50} values for inhibitors of CYP26A1
IC_{50} values were obtained from the fits of the data shown in Figs. 5 and 6.

Compound	IC_{50} or K_d (S.E.)
	μM
R116010	0.0043 (0.0007)
R115866	0.0051 (0.0008)
CD1530	0.53 (1.9)
Ketoconazole	0.55 (1.3)
L-165,041	1.7 (1.6)
Liarozole	2.1 (1.1)
CS5	2.6 (1.3)[a]
TTNPB	3.7 (1.6)
Rosiglitazone	4.2 (1.3)
Pioglitazone	8.6 (1.2)

[a] The IC_{50} value is determined as 50% inhibition of the maximum 71% inhibition observed.

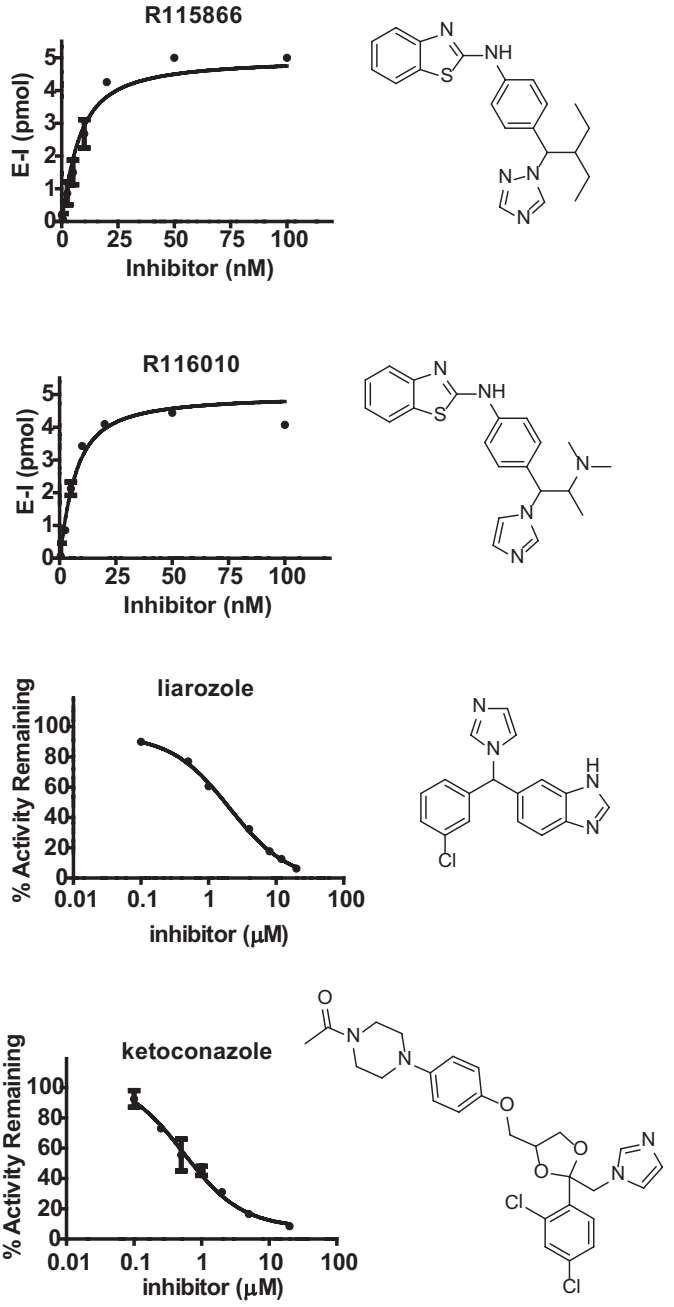

Fig. 5. Determination of IC_{50} and K_d values for azole inhibitors of CYP26A1 and the relevant structures. IC_{50} values were calculated by incubating 5 pmol of CYP26A1, 10 pmol of reductase, 100 nM 9-*cis*-RA, and at least five concentrations of inhibitor. The percentage activity remaining or concentration of the enzyme inhibitor complex was calculated and plotted against the inhibitor concentration. The Morrison equation (eq. 2) was fit to the R115866 and R116010 data. Equation 1 was fitted to the liarozole and ketoconazole data.

suggesting that both substrates have multiple binding orientations in the CYP26A1 active site. Despite the formation of two metabolites from 9-*cis*-RA, 9-*cis*-RA hydroxylation is a better probe for testing CYP26A1 inhibition than atRA metabolism. The key advantages of using 9-*cis*-RA instead of atRA for measuring inhibition of CYP26A1 are the lower binding affinity of 9-*cis*-RA to CYP26A1 and lack of substantial sequential metabolism and product depletion.

With use of 9-*cis*-RA hydroxylation as a probe, 21 potential inhibitors of CYP26A1 were identified from a wide variety of compounds. With the exception of ketoconazole, the compounds selected from classic P450 substrates and inhibitors either did not inhibit CYP26A1 or inhibited it weakly, demonstrating that CYP26A1 has high ligand selectivity. In addition, with the exception of ketoconazole, the compounds with high affinity (<1 μM IC_{50}) for CYP26A1 were designed either as inhibitors of RA metabolism or as RAR agonists using atRA as the lead structure.

Overall, the RAR agonists had lower affinity for CYP26A1 than for RAR isoforms. An exception was CD1530, which had a binding affinity toward CYP26A1 similar to that reported for RARγ (Thacher et al., 2000) and higher affinity for CYP26A1 than for RARα and RARβ isoforms. In cell systems, CD1530 is expected to inhibit CYP26A1 at concentrations similar to those required for RARγ activation. TTNPB and AM 580 had lower binding affinities toward CYP26A1 than those reported for RAR isoforms (Thacher et al., 2000), but it is possible that when used in cell systems these compounds also inhibit CYP26A1. This is an important finding because CYP26A1 inhibition leading to increased concentrations of atRA in cells simultaneously with RAR activation could confound results in RAR activation assays and mask the mechanism of cellular effects.

Our findings confirm previous studies showing that R115866 and R116010 inhibit atRA metabolism with high affinity. R115866 had IC_{50} values of 4 and 5 nM when tested

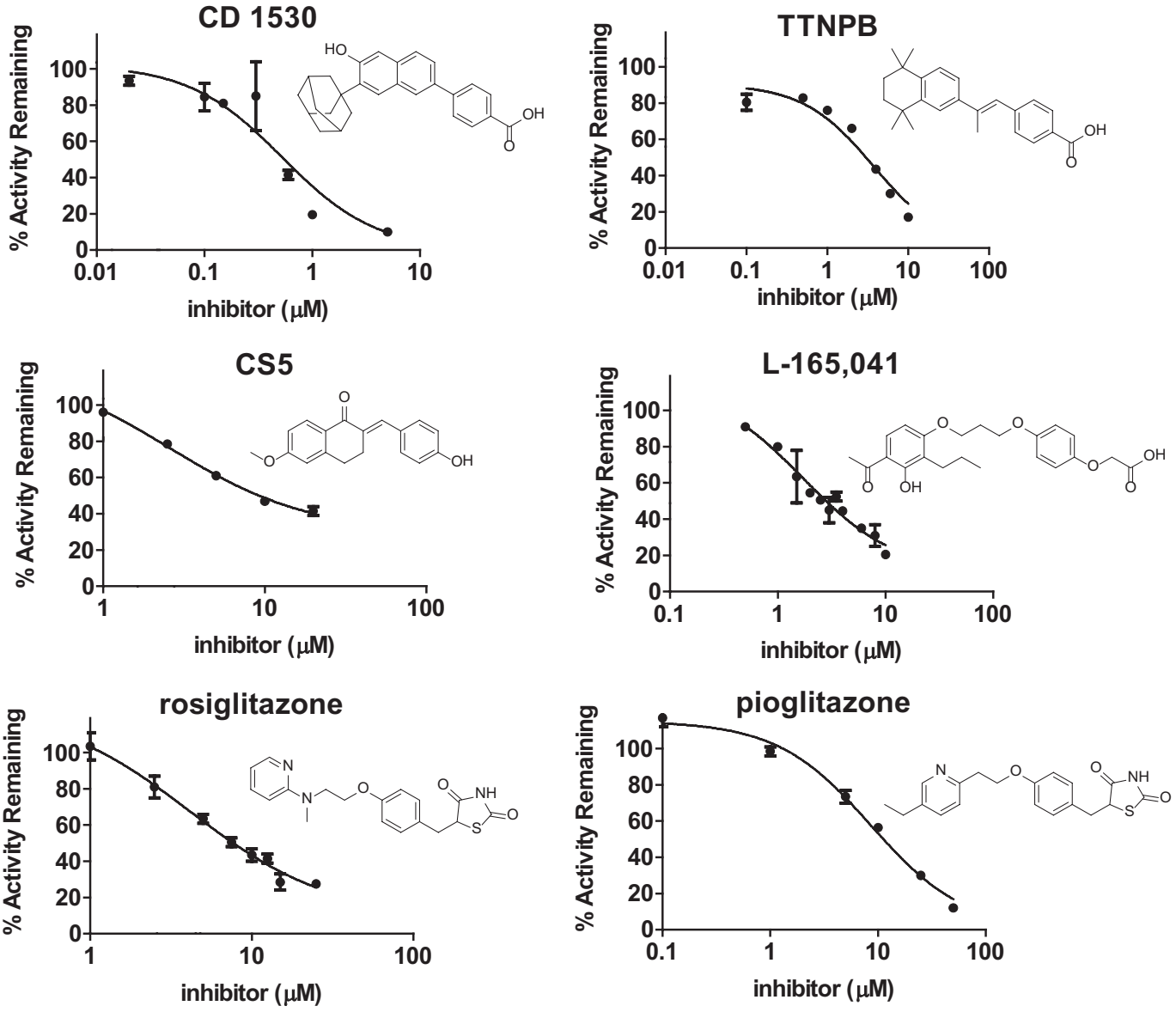

Fig. 6. Determination of IC_{50} values for PPAR and RAR ligands and CS5 toward CYP26A1-mediated 9-*cis*-RA oxidation. Insets, structures of the inhibitors. IC_{50} values were calculated by incubating 5 pmol of CYP26A1, 10 pmol of reductase, 100 nM 9-*cis*-RA, and at least five concentrations of inhibitor. The percentage activity remaining was calculated and plotted against inhibitor concentration and eq. 1 was fitted to the data.

in yeast and MCF-7 cells expressing CYP26A1, respectively (Stoppie et al., 2000), and R116010 had an IC_{50} of 8.7 nM in human T47D breast cancer cells induced with atRA (Van Heusden et al., 2002). The inhibitory potency of ketoconazole toward CYP26A1 in this study was much higher (IC_{50} = 0.5 μM) than previously observed (IC_{50} = 18 and 12 μM in rat liver microsomes and MCF-7 cells, respectively). The inhibitory potency of CS5 was in good agreement with previous studies. The IC_{50} value for CS5 was >20 μM when tested in rat liver microsomes and 7 μM when tested in atRA-induced MCF-7 cells (Yee et al., 2005). In MCF-7 cells and rat liver microsomes, CS6 was a more potent inhibitor than CS5 (IC_{50} = 0.4 and 5 μM in rat liver microsomes and MCF-7 cells, respectively) and was suggested to have more broad inhibition potential than CS5 (Yee et al., 2005). In our study, CS6 inhibited CYP26A1 activity <20% when tested at 10 μM in comparison to 50% inhibition by CS5. A possible explanation for these discrepancies is the contribution of other enzymes to atRA metabolism in rat liver microsomes and/or MCF-7 cells or differences in nonspecific binding of the inhibitors in different systems. The differences in inhibitory potencies between the systems highlight the need for determining initial inhibition constants using a single enzyme system. This is especially important when reliable selective probe substrates are not available for the specific P450 isoform. Because atRA is metabolized by multiple P450 enzymes (Thatcher et al., 2010), the contribution of each isoform is expected to vary between different tissues and cell types. At present, the predominant CYP26 isoform expressed in MCF-7 cells and the selectivity of the inhibitors for different CYP26 isoforms are unknown.

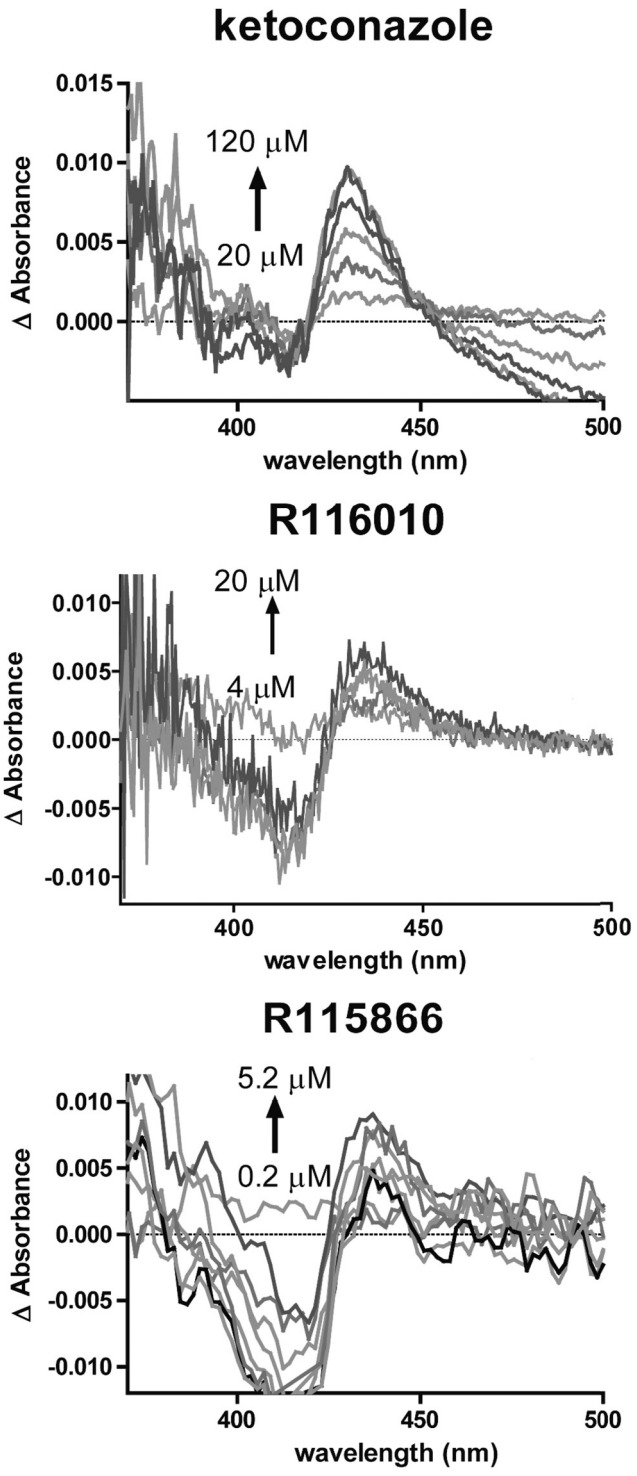

Fig. 7. Ligand-induced difference spectra for ketoconazole, R116010, and R115866 binding to CYP26A1. All spectra were recorded as described under *Materials and Methods*.

The result that ketoconazole is 4-fold more potent CYP26A1 inhibitor than liarozole is in contrast with what was expected from in vivo findings (Van Wauwe et al., 1990). In rats, when administered at similar doses, liarozole caused an approximately 3-fold increase in atRA AUC, whereas ketoconazole only increased atRA concentrations 1.5-fold (Van Wauwe et al., 1990). This discrepancy is most likely due to different circulating free concentrations of ketoconazole and liarozole resulting from different plasma protein binding, clearance, and volume of distribution. In agreement with our data, both liarozole and ketoconazole have been shown to inhibit atRA metabolism in vitro in hamster or rat liver microsomes (Van Wauwe et al., 1988, 1992). In addition, no potent CYP26A1 inhibition was observed by itraconazole in this study, similar to the data that itraconazole did not inhibit atRA metabolism in vivo in rats (Van Wauwe et al., 1990).

The finding that ketoconazole is a potent inhibitor of CYP26A1 is consistent with clinical findings that the dose of atRA needs to be decreased when atRA is coadministered with ketoconazole or fluconazole. When ketoconazole was administered on day 28 of atRA therapy, a 72% increase in plasma AUC of atRA was observed (Rigas et al., 1993), suggesting a <50% decrease in the clearance of atRA. The finding that fluconazole (C_{max} = 43.6 μM) (Debruyne and Ryckelynck, 1993) is a weak CYP26A1 inhibitor (IC_{50} >10 μM) does not explain the 2- to 4-fold increase in atRA AUC (Schwartz et al., 1995) or a need to decrease atRA dose by 70% (Vanier et al., 2003) after fluconazole administration. This finding suggests that CYP26A1 is not the only enzyme clearing atRA in humans. It is possible that fluconazole causes the interaction by inhibiting other CYP26 isoforms or CYP2C and CYP3A enzymes.

It is surprising that the PPARγ and PPARβ/δ agonists pioglitazone, rosiglitazone, and L165,041 inhibited CYP26A1 with potency similar to that for liarozole. In previous studies, pioglitazone and rosiglitazone were found to induce CYP26B1 mRNA in HepG2 cells (Tay et al., 2010), but they have not previously been shown to affect atRA metabolism. Because

pioglitazone and rosiglitazone plasma concentrations reach low micromolar (C_{max}) values after clinical administration, it is possible that these drugs cause weak-to-moderate inhibition of atRA metabolism in vivo. This is of interest because pioglitazone and rosiglitazone are used for treatment of diabetes, and 9-*cis*-RA was recently shown to play a role in regulation of blood glucose (Kane et al., 2010). It is possible that inhibition of 9-*cis*-RA metabolism in the pancreas also plays a role in the activity of pioglitazone and rosiglitazone.

In conclusion, this study shows that CYP26A1 has high ligand selectivity but can be inhibited by retinoids and other structurally related drugs. This study also shows that 9-*cis*-RA and 13-*cis*-RA are substrates for CYP26A1, suggesting that CYP26A1 has a role in inactivating bioactive retinoids. This finding may be important in further understanding of retinoid biochemistry. Further studies screening a larger panel of retinoids and RAR agonists are needed to determine the extent of ligand overlap between RAR isoforms and CYP26 enzymes. On the basis of the data presented, RAR, PPAR, and CYP26A1 have considerable ligand overlap, suggesting that inhibition of CYP26A1, leading to increased atRA concentrations, could contribute to the biological activity of RAR and PPAR agonists.

Acknowledgments

We thank Jessica Tay, Dr. Vaishali Dixit, and Dr. Alex Zelter for assistance with CYP26 expression and in conducting preliminary experiments of CYP26A1 inhibition and metabolism and Dr. Justin D. Lutz for assistance with the LC-MS/MS experiments. We also thank Dr. William Atkins and Rob Foti for assistance with the selection of broad range substrates to screen as potential inhibitors of CYP26.

Authorship Contributions

Participated in research design: Thatcher, Nelson, and Isoherranen.

Conducted experiments: Thatcher, Buttrick, Shaffer, and Isoherranen.

Contributed new reagents or analytic tools: Shimshoni and Goodlett.

Performed data analysis: Thatcher, Buttrick, Shaffer, Goodlett, Nelson, and Isoherranen.

Wrote or contributed to the writing of the manuscript: Thatcher, Shaffer, Nelson, and Isoherranen.

References

Alder A, Bigler P, Werck-Reichhart D, and Al-Babili S (2009) In vitro characterization of *Synechocystis* CYP120A1 revealed the first nonanimal retinoic acid hydroxylase. *FEBS J* **276:**5416–5431.

Altucci L, Leibowitz MD, Ogilvie KM, de Lera AR, and Gronemeyer H (2007) RAR and RXR modulation in cancer and metabolic disease. *Nat Rev Drug Discov* **6:**793–810.

Barua RK and Barua AB(1964) Vitamin A acid from retinene. *Biochem J* **92:**21C–22C.

Blomhoff R and Blomhoff HK (2006) Overview of retinoid metabolism and function. *J Neurobiol* **66:**606–630.

Chithalen JV, Luu L, Petkovich M, and Jones G (2002) HPLC-MS/MS analysis of the products generated from all-*trans*-retinoic acid using recombinant human CYP26A. *J Lipid Res* **43:**1133–1142.

Debruyne D and Ryckelynck JP (1993) Clinical pharmacokinetics of fluconazole. *Clin Pharmacokinet* **24:**10–27.

Duester G (2008) Retinoic acid synthesis and signaling during early organogenesis. *Cell* **134:**921–931.

Garattini E, Gianni M, and Terao M (2007) Retinoids as differentiating agents in oncology: a network of interactions with intracellular pathways as the basis for rational therapeutic combinations. *Curr Pharm Des* **13:**1375–1400.

Gomaa MS, Yee SW, Milbourne CE, Barbera MC, Simons C, and Brancale A (2006) Homology model of human retinoic acid metabolising enzyme cytochrome P450 26A1 (CYP26A1): active site architecture and ligand binding. *J Enzyme Inhib Med Chem* **21:**361–369.

Jacobs S, Lie DC, DeCicco KL, Shi Y, DeLuca LM, Gage FH, and Evans RM (2006) Retinoic acid is required early during adult neurogenesis in the dentate gyrus. *Proc Natl Acad Sci USA* **103:**3902–3907.

Kane MA, Folias AE, Pingitore A, Perri M, Obrochta KM, Krois CR, Cione E, Ryu JY, and Napoli JL (2010) Identification of 9-*cis*-retinoic acid as a pancreas-specific autacoid that attenuates glucose-stimulated insulin secretion. *Proc Natl Acad Sci USA* **107:**21884–21889.

Kane MA, Folias AE, Wang C, and Napoli JL (2008) Quantitative profiling of endogenous retinoic acid in vivo and in vitro by tandem mass spectrometry. *Anal Chem* **80:**1702–1708.

Karlsson M, Strid A, Sirsjo A, and Eriksson LA (2008) Homology models and molecular modeling of human retinoic acid metabolizing enzymes cytochrome P450 26A1 (CYP26A1) and P450 26B1 (CYP26B1). *J Chem Theory Comput* **4:**1021–1027.

Kühnel K, Ke N, Cryle MJ, Sligar SG, Schuler MA, and Schlichting I(2008) Crystal structures of substrate-free and retinoic acid-bound cyanobacterial cytochrome P450 CYP120A1. *Biochemistry* **47:**6552–6559.

Lutz JD, Dixit V, Yeung CK, Dickmann LJ, Zelter A, Thatcher JE, Nelson WL, and Isoherranen N (2009) Expression and functional characterization of cytochrome P450 26A1, a retinoic acid hydroxylase. *Biochem Pharmacol* **77:**258–268.

Muindi J, Frankel SR, Miller WH Jr, Jakubowski A, Scheinberg DA, Young CW, Dmitrovsky E, and Warrell RP Jr (1992) Continuous treatment with all-*trans* retinoic acid causes a progressive reduction in plasma drug concentrations: implications for relapse and retinoid "resistance" in patients with acute promyelocytic leukemia. *Blood* **79:**299–303.

Mulvihill MJ, Kan JL, Beck P, Bittner M, Cesario C, Cooke A, Keane DM, Nigro AI, Nillson C, Smith V, et al. (2005) Potent and selective [2-imidazol-1-yl-2-(6-alkoxy-naphthalen-2-yl)-1-methyl-ethyl]-dimethyl-amines as retinoic acid metabolic blocking agents (RAMBAs). *Bioorg Med Chem Lett* **15:**1669–1673.

Njar VC, Gediya L, Purushottamachar P, Chopra P, Vasaitis TS, Khandelwal A, Mehta J, Huynh C, Belosay A, and Patel J (2006) Retinoic acid metabolism blocking agents (RAMBAs) for treatment of cancer and dermatological diseases. *Bioorg Med Chem* **14:**4323–4340.

Patel JB, Huynh CK, Handratta VD, Gediya LK, Brodie AM, Goloubeva OG, Clement OO, Nanne IP, Soprano DR, and Njar VC (2004) Novel retinoic acid metabolism blocking agents endowed with multiple biological activities are efficient growth inhibitors of human breast and prostate cancer cells in vitro and a human breast tumor xenograft in nude mice. *J Med Chem* **47:**6716–6729.

Petkovich M, Brand NJ, Krust A, and Chambon P (1987) A human retinoic acid receptor which belongs to the family of nuclear receptors. *Nature* **330:**444–450.

Ren JH, Xiong XQ, Sha Y, Yan MC, Lin B, Wang J, Jing YK, Zhao DM, and Cheng MS (2008) Structure prediction and R115866 binding study of human CYP26A1: homology modelling, fold recognition, molecular docking and MD simulations. *Mol Simulation* **34:**337–346.

Rigas JR, Francis PA, Muindi JR, Kris MG, Huselton C, DeGrazia F, Orazem JP, Young CW, and Warrell RP Jr (1993) Constitutive variability in the pharmacokinetics of the natural retinoid, all-trans-retinoic acid, and its modulation by ketoconazole. *J Natl Cancer Inst* **85:**1921–1926.

Schwartz EL, Hallam S, Gallagher RE, and Wiernik PH (1995) Inhibition of all-*trans*-retinoic acid metabolism by fluconazole in vitro and in patients with acute promyelocytic leukemia. *Biochem Pharmacol* **50:**923–928.

Sonneveld E, van den Brink CE, van der Leede BM, Schulkes RK, Petkovich M, van der Burg B, and van der Saag PT (1998) Human retinoic acid (RA) 4-hydroxylase (CYP26) is highly specific for all-*trans*-RA and can be induced through RA receptors in human breast and colon carcinoma cells. *Cell Growth Differ* **9:**629–637.

Stoppie P, Borgers M, Borghgraef P, Dillen L, Goossens J, Sanz G, Szel H, Van Hove C, Van Nyen G, Nobels G, et al. (2000) R115866 inhibits all-*trans*-retinoic acid metabolism and exerts retinoidal effects in rodents. *J Pharmacol Exp Ther* **293:**304–312.

Taimi M, Helvig C, Wisniewski J, Ramshaw H, White J, Amad M, Korczak B, and Petkovich M (2004) A novel human cytochrome P450, CYP26C1, involved in metabolism of 9-cis and all-*trans* isomers of retinoic acid. *J Biol Chem* **279:**77–85.

Tang XH and Gudas LJ (2011) Retinoids, retinoic acid receptors, and cancer. *Annu Rev Pathol* **6:**345–364.

Tay S, Dickmann L, Dixit V, and Isoherranen N (2010) A comparison of the roles of peroxisome proliferator-activated receptor and retinoic acid receptor on CYP26 regulation. *Mol Pharmacol* **77:**218–227.

Thacher SM, Vasudevan J, and Chandraratna RA (2000) Therapeutic applications for ligands of retinoid receptors. *Curr Pharm Des* **6:**25–58.

Thatcher JE, Zelter A, and Isoherranen N (2010) The relative importance of CYP26A1 in hepatic clearance of all-*trans* retinoic acid. *Biochem Pharmacol* **80:**903–912.

van der Leede BM, van den Brink CE, Pijnappel WW, Sonneveld E, van der Saag PT, and van der Burg B (1997) Autoinduction of retinoic acid metabolism to polar derivatives with decreased biological activity in retinoic acid-sensitive, but not in retinoic acid-resistant human breast cancer cells. *J Biol Chem* **272:**17921–17928.

Van Heusden J, Van Ginckel R, Bruwiere H, Moelans P, Janssen B, Floren W, van der Leede BJ, van Dun J, Sanz G, Venet M, et al. (2002) Inhibition of all-TRANS-retinoic acid metabolism by R116010 induces antitumour activity. *Br J Cancer* **86:**605–611.

Van Wauwe J, Van Nyen G, Coene MC, Stoppie P, Cools W, Goossens J, Borghgraef P, and Janssen PA (1992) Liarozole, an inhibitor of retinoic acid metabolism, exerts retinoid-mimetic effects in vivo. *J Pharmacol Exp Ther* **261:**773–779.

Van Wauwe JP, Coene MC, Goossens J, Cools W, and Monbaliu J (1990) Effects of cytochrome P-450 inhibitors on the in vivo metabolism of all-*trans*-retinoic acid in rats. *J Pharmacol Exp Ther* **252:**365–369.

Van Wauwe JP, Coene MC, Goossens J, Van Nijen G, Cools W, and Lauwers W (1988) Ketoconazole inhibits the in vitro and in vivo metabolism of all-*trans*-retinoic acid. *J Pharmacol Exp Ther* **245:**718–722.

Vanier KL, Mattiussi AJ, and Johnston DL (2003) Interaction of all-trans-retinoic acid with fluconazole in acute promyelocytic leukemia. *J Pediatr Hematol Oncol* **25:**403–404.

White JA, Beckett-Jones B, Guo YD, Dilworth FJ, Bonasoro J, Jones G, and Petkovich M (1997) cDNA cloning of human retinoic acid-metabolizing enzyme

(hP450RAI) identifies a novel family of cytochromes P450. *J Biol Chem* **272:** 18538–18541.

White JA, Guo YD, Baetz K, Beckett-Jones B, Bonasoro J, Hsu KE, Dilworth FJ, Jones G, and Petkovich M (1996) Identification of the retinoic acid-inducible all-*trans*-retinoic acid 4-hydroxylase. *J Biol Chem* **271:**29922–29927.

Wouters W, van Dun J, Dillen A, Coene MC, Cools W, and De Coster R (1992) Effects of liarozole, a new antitumoral compound, on retinoic acid-induced inhibition of cell growth and on retinoic acid metabolism in MCF-7 human breast cancer cells. *Cancer Res* **52:**2841–2846.

Yee SW, Jarno L, Gomaa MS, Elford C, Ooi LL, Coogan MP, McClelland R, Nicholson RI, Evans BA, Brancale A, et al. (2005) Novel tetralone-derived retinoic acid metabolism blocking agents: synthesis and in vitro evaluation with liver microsomal and MCF-7 CYP26A1 cell assays. *J Med Chem* **48:**7123–7131.

Address correspondence to: Dr. Nina Isoherranen, Department of Pharmaceutics, Box 357610, University of Washington, Seattle, WA 98195. E-mail: ni2@u.washington.edu